The Chemistry of Iron Carbonyl Sulfide and Selenide Anions

Russell L. Holliday, Lisa C. Roof, Beverly Hargus, Donna M. Smith, Paul T. Wood, William T. Pennington, and Joseph W. Kolis*

Department of Chemistry, Clemson University, Clemson, South Carolina 29634-1905

Received July 8, 1994[⊗]

The reactions of $Fe(CO)_5$ with polysulfides and polyselenides of various chain lengths and stoichiometries were investigated. It was found that $Fe(CO)_5$ must always be present in excess relative to the polychalcogenide chain, or immediate decomposition would result. Conversely, if $Fe(CO)_5$ is present in large excess $[Fe_3(CO)_9(\mu_3\text{-}E)]^{2-}$ (E = S, Se) is formed in excellent yield. This was isolated in very good yield as its $[Ph_4P]^+$ salt. The salt $[Ph_4P]_2[Fe_3(CO)_9(\mu_3\text{-}Se]$, **Ib**, crystallizes in the triclinic space group $P\bar{1}$; $a = 11.580(4)$ Å, $b = 12.369(3)$ Å, $c = 19.707(4)$ Å, $\alpha = 88.18(2)°$, $\beta = 81.78(2)°$, $\gamma = 71.32(2)°$, $V = 2646(1)$ Å^3, $Z = 2$, $R = 0.0322$, $R_w = 0.0358$. As the ratio and chain length of polychalcogenide are increased, there is increased oxidation of the iron centers, leading to clusters with formulas $[Fe_5(CO)_{14}(\mu_3\text{-}E)_2]^{2-}$ and $[Fe_6(CO)_{12}E_6]^{2-}$ (E = S, Se) successively. The salt $[n\text{-}Bu_4N]_2[Fe_5(CO)_{14}(\mu_3\text{-}S)_2]$, **II**, crystallizes in the monoclinic space group $P2_1/c$; $a = 33.284(7)$ Å, $b = 18.769(4)$ Å, $c = 18.704(4)$ Å, $\beta = 90.945(5)°$, V =11683(10) Å^3, $Z = 8$, $R = 0.0987$, $R_w = 0.1179$. The salt $[Ph_4P]_2[Fe_5(CO)_{14}(\mu_3\text{-}Se)_2]$, **III**, crystallizes in the triclinic space group $P\bar{1}$; $a = 12.951(4)$ Å, $b = 13.155(6)$ Å, $c = 20.729(8)$ Å, $\alpha = 98.01(3)°$, $\beta = 94.25(3)°$, $\gamma = 115.77(3)°$, $V = 3113(2)$ Å^3, $Z = 2$, $R = 0.0742$, $R_w = 0.0883$. The salt $[Et_4N]_2[Fe_6(CO)_{12}Se_6]$, **IVb**, crystallizes in the monoclinic space group $P2_1/c$; $a = 12.134(2)$ Å, $b = 12.753(2)$ Å, $c = 16.058(2)$ Å, $\beta = 112.51(2)°$, V =2348.8(5) Å^3, $Z = 2$, $R = 0.0307$, $R_w = 0.0335$. The cluster $[Fe_6(CO)_{12}E_6]^{2-}$ could be used as a $[Fe_2(CO)_6E]^{2-}$ transfer group for M(II) salts, leading to formation of $[MFe_4(CO)_{12}S_4]^{2-}$ (M = Ni, Pd). The salt $[Ph_4P]_2[\{Fe_2(CO)_6(\mu_3\text{-}S)_2\}_2Ni]\cdot CH_2Cl_2$, **Va**, crystallizes in the triclinic space group $P\bar{1}$; $a = 11.270(4)$ Å, $b = 12.038(5)$ Å, $c = 12.664(5)$ Å, $\alpha = 79.53(3)°$, $\beta = 82.55(3)°$, $\gamma = 89.32(3)°$, $V = 1675(1)$ Å^3, $Z = 1$, $R = 0.0543$, $R_w = 0.0699$. Cyclic voltammograms were obtained for all these clusters, identifying other stable oxidation states.

Introduction

The last several years have seen an expansion of interest in the comparative coordination chemistry of polyselenide and -telluride ligands versus that of polysulfides.[1] The driving force for this interest is the fact that the heavier polychalcogenides often display substantially different structures and reactivity in the presence of transition metal ions than do their better understood sulfur counterparts.[2] Recently we have been specifically focusing on the coordination chemistry of polychalcogenide anions with metal carbonyls. We have found that this chemistry is much richer and more complex than originally envisioned.[3] In particular, when a polychalcogenide chain E_n^{2-} (E = S, Se, Te) ($n = 2-6$) coordinates to a low-valent metal carbonyl center, intramolecular electron transfer often occurs from the metal center into one or more chalcogen–chalcogen bonds. This leads to reductive cleavage of the polychalcogenide chain and oxidation of the metal center, with concomitant loss of CO ligands. The oxidation of the metal center can result in complete loss of carbonyls with formation of binary metal chalcogenide anions or, more often, partial oxidation of the metal center and cluster formation. The degree of clusterification can often be controlled by the relative ratios of the polychalcogenide and parent metal carbonyl.

Recently we found that the reaction of polytellurides with iron carbonyls leads to a rich array of novel cluster compounds, the identities of which can be controlled by the stoichiometries and composition of the starting telluride anions. For example, reaction of $Fe(CO)_5$ with the shortest member of the series, Te^{2-}, leads to formation of $[Fe_3(CO)_9(\mu_3\text{-}Te)]^{2-}$ in nearly quantitative yield.[4] However, reaction of $Fe(CO)_5$ with increasing amounts of Te_4^{2-} leads to formation of $[Fe_5(CO)_{14}Te_4]^{2-}$,[5a] $[Fe_6(CO)_{16}Te_6]^{2-}$,[5b] and $[Fe_8(CO)_{20}Te_{10}]^{2-}$,[5a] successively. These clusters are characterized by the increasing degree of oxidation of the iron centers, which is consistent with our view that the polychalcogenides are actually acting as oxidants toward the metal centers. The structure of $[Fe_8(CO)_{20}Te_{10}]^{2-}$ was particularly intriguing, given the similarity of the shape of its heavy element framework to iron sulfide clusters of biological significance.[6] There have been a number of iron carbonyl sulfides and selenides reported in the literature, but the reactions of these polychalcogenide anions with $Fe(CO)_5$ has not been examined in a systematic manner. Thus we investigated these reactions to try to isolate other iron dicubane clusters. In this paper we report the reactions of $Fe(CO)_5$ with several polysulfide and -selenide anions, along with their structural and spectroscopic characterization. We also report the preliminary

* To whom correspondence should be addressed. E-mail: KJOSEPH@Clemson.edu.

⊗ Abstract published in *Advance ACS Abstracts,* April 15, 1995.

(1) (a) Roof, L. C.; Kolis, J. W. *Chem. Rev.* **1993**, *93*, 1037. (b) Ansari, M. A.; Ibers, J. A. *Coord. Chem. Rev.* **1990**, *100*, 223. (c) Kanatzidis, M. G. *Comments Inorg. Chem.***1990**, *10*, 161. (d) Gysling, H. J. *Coord. Chem. Rev.* **1982**, *42*,133. (e) Kanatzidis, M. G.; Huang, S. P. *Coord. Chem. Rev.* **1994**, *130*, 509.

(2) (a) Draganjac, M.; Rauchfuss, T. B. *Angew. Chem., Int. Ed. Engl.* **1985**, *24*, 742. (b) Müller, A.; Diemann, E. *Adv. Inorg. Chem.* **1987**, *31*, 89. (c) Müller, A.; Diemann, E. *Comprehensive Coordination Chemistry;* Wilkinson, G., Ed.; Pergamon Press: Oxford, U.K., 1987; Vol. 2, p 515. (d) Wachter, J. *Angew. Chem., Int. Ed. Engl.* **1989**, *28*, 1613. (e) Harmer, M. A.; Halbert, T. R.; Pan, W.-H.; Coyle, C. L.; Cohen, S. A.; Stiefel, E. I. *Polyhedron* **1986**, *5*, 341. (f) Coucouvanis, D.; Hadjikyriacou, A.; Draganjac, M.; Kanatzidis, M. G.; Ileperuma, O. *Polyhedron* **1986**, *5*, 349

(3) Kolis, J. W. *Coord. Chem. Rev.* **1990**, *105*, 195.

(4) Roof, L. C.; Smith, D. M.; Drake, G. W.; Pennington, W. T.; Kolis, J. W. *Inorg. Chem.* **1995**, *34*, 337.

(5) (a) Roof, L. C.; Pennington, W. T.; Kolis, J. W. *Angew. Chem., Int. Ed. Engl.* **1992**, *31*, 913. (b) Roof, L. C.; Pennington, W. T.; Kolis, J. W. Unpublished work.

(6) (a) Holm, R. H.; Ciurli, S.; Weigel, J. A. *Prog. Inorg. Chem.* **1990**, *38*, 2. (b) Lindahl, P. A.; Kovacs, J. A. *J. Cluster Sci.* **1990**, *1*, 29. (c) Coucouvanis, D. *Acc. Chem. Res.* **1991**, *24*, 1.

0020-1669/95/1334-4392$09.00/0

investigation of their reactions with various other metal complexes to form new heterometallic clusters.

Experimental Section

All reactions were performed under argon using standard air-sensitive techniques. Solvents were dried and degassed by conventional methods and all solids were handled in a drybox under argon. Metal carbonyls and other standard reagents were obtained from commercial houses and used as received. The alkali metal chalcogenides K_2E_n (E = S, Se) ($n = 1-4$) were prepared by stirring the elements in the appropriate stoichiometries in liquid NH_3 for 4 h at −78 °C followed by evaporation of the ammonia. IR spectra were obtained in purged CaF_2 cells or as Nujol mulls in polyethylene bags. Microanalyses were obtained from Atlantic Microlabs, Norcross, GA. Cyclic voltammograms (CVs) were obtained with an EG&G PAR 273 potentiostat/galvanostat in acetonitrile, at a sweep rate of 100 mV/s, with platinum disk working and auxiliary electrodes and potentials referenced to SCE. The CVs were recorded under a blanket of dry nitrogen. The supporting electrolyte was 0.1M tetrabutylammonium hexafluorophosphate.

Synthesis of $[Ph_4P]_2[Fe_3(CO)_9(\mu_3\text{-}S)]$, Ia. In a typical reaction, 0.14 g (3.6 mmol) of K and 0.06 g (1.9 mmol) of S powder were added to 10 mL of DMF, and the mixture was allowed to stir rapidly at 23 °C until the solids dissolved. To the yellow-orange solution was added 0.72 mL (5.5 mmol) of $Fe(CO)_5$ and the mixture heated to 100 °C in an oil bath for 2 h. To the red-brown solution was added 1.52 g (3.62 mmol) of Ph_4PBr, and the mixture was stirred for 20 min until the solids dissolved. The DMF was removed under vacuum, and the dark oil was extracted with 10 mL of CH_2Cl_2. The solution was filtered, and the filtrate was layered with 10 mL of diethyl ether. Storage overnight at 23 °C resulted in formation of red plates and needles of the product in good yield (67% based on Fe). Anal. Calcd for $C_{57}H_{40}O_9P_2Fe_3S$: C, 60.56; H, 3.54. Found: C, 60.00; H, 3.63. IR (cm^{-1}, DMF) (ν_{CO}): 1997 (m), 1927 (s), 1901 (s), 1871 (m). IR (cm^{-1}, Nujol mull): 617 (m), 598 (s), 578 (s), 525 (s), 461 (m), 444 (w), 397 (w), 321 (m).

Synthesis of $[Ph_4P]_2[Fe_3(CO)_9(\mu_3\text{-}Se)]$, Ib. In a reaction similar to that described above, 0.10 g (2.5 mmol) of K and 0.10 g of (1.3 mmol) gray Se powder were combined in DMF. To the orange-brown solution was added 0.50 mL (3.8 mmol) of $Fe(CO)_5$, and the mixture was heated to 100 °C for 2 days. To the reaction mixture was added 1.07 g (2.55 mmol) of Ph_4PBr, and the dark red solution was worked up as described above. Layering with 10 mL of diethyl ether and storage overnight at 4 °C resulted in formation of red brown parallelepipeds of the product in 48% yield. Anal. Calcd for $C_{57}H_{40}O_9P_2Fe_3Se$: C, 58.14; H, 3.40. Found: C, 57.91; H, 3.41. IR (cm^{-1}, DMF) (ν_{CO}): 1994 (m), 1926 (s), 1898 (m), 1870 (m). IR (cm^{-1}, Nujol mull): 617 (m), 600 (s), 582 (s), 525 (s), 461 (m), 444 (w), 396 (m), 320 (m). A small amount (3% yield) of $[Ph_4P]_2[Fe_5(CO)_{14}(\mu_3\text{-}Se)_2]$ can be manually separated from the mixture as well-formed dark brown needles.

Synthesis of $[n\text{-}Bu_4N]_2[Fe_5(CO)_{14}(\mu_3\text{-}S)_2]$, II. A Schlenk flask was charged with 0.10 g (0.49 mmol) of K_2S_4, and 10 mL of DMF was added. The solution was stirred until the polysulfide was dissolved to generate a blue-green solution. A 0.45 mL (3.4 mmol) aliquot of $Fe(CO)_5$ was added and the mixture heated to 100 °C for 1.5 h. To the dark brown solution was added 0.40 g (1.24 mmol) of n-Bu_4NBr with stirring and the DMF removed under vacuum. Extraction of the dark brown oil with 10 mL of CH_2Cl_2 was followed by filtration and layering with 10 mL of diethyl ether. Overnight storage at 4 °C resulted in formation of black square plates of the product in 36% yield. Anal. Calcd for $C_{46}H_{72}O_{14}N_2Fe_5S_2$: C, 45.28; H, 5.91; N, 2.29. Found: C, 45.28; H, 6.02; N, 2.38. IR (cm^{-1}, DMF) (ν_{CO}): 1994 (s), 1977 (s), 1964 (s), 1940 (m), 1917 (m). IR (cm^{-1}, Nujol mull): 617 (m), 602 (s), 573 (s), 555 (m), 507 (m), 459 (w), 444 (m), 385 (m).

Synthesis of $[Ph_4P]_2[Fe_5(CO)_{14}(\mu_3\text{-}Se)_2]$, III. This product could be isolated from the reaction to form $[Ph_4P]_2[Fe_3(CO)_9(\mu_3\text{-}Se)]$ by manual separation of the obviously darker crystals from the red $[Ph_4P]_2[Fe_3(CO)_9(\mu_3\text{-}Se)]$. However they only appeared in this reaction in very low yield. The product could be prepared in a reasonable yield by adding 0.033 g (0.84 mmol) of K and 0.067 g (0.86 mmol) of gray Se powder to 10 mL of DMF and stirring overnight until the solids dissolved. To the green polyselenide solution was added 0.28 mL (2.1 mmol) of $Fe(CO)_5$ and the solution stirred at 100 °C for 18 h. After addition of 0.36 g of Ph_4PBr (0.86 mmol) to the brown solution, the solvent was removed, the oil extracted with CH_2Cl_2, and the extract layered as described above. Storage at 23 °C resulted in formation of dark brown polyhedra in 11% yield. Anal. Calcd for $C_{62}H_{40}O_{14}P_2Fe_5Se_2$: C, 49.37; H, 2.65. Found: C, 49.35; H, 2.69. IR (cm^{-1}, DMF) (ν_{CO}): 2029 (m), 1992 (s), 1976 (s), 1962 (s), 1936 (m), 1916 (m). IR (cm^{-1}, Nujol mull): 614 (m), 604 (s), 585 (s), 528 (s), 448 (s).

Synthesis of $[Et_4N]_2[Fe_6(CO)_{12}S_6]$, IVa. A Schlenk flask was charged with 0.10 g (0.49 mmol) of K_2S_4 and 0.031 g (0.97mmol) of elemental S, and 10 mL DMF was added. The solution was stirred until the polysulfide was dissolved, forming a green solution. A 0.38 mL (2.9 mmol) aliquot of $Fe(CO)_5$ was added and the mixture stirred at 23 °C for 16 h. To the dark brown solution was added 0.20 g (0.95 mmol) of Et_4NBr with stirring and the DMF removed under vacuum. Extraction with 10 mL of CH_2Cl_2 and layering with 10 mL of diethyl ether, followed by overnight storage at 4 °C, resulted in formation of burgundy red hexagonal plates of the product in 22% yield. Anal. Calcd for $C_{28}H_{40}O_{12}N_2Fe_6S_6$: C, 29.90; H, 3.56; N, 2.49. Found: C, 29.86; H, 3.71; N, 2.49. IR (cm^{-1}, DMF) (ν_{CO}): 2039 (s), 2010 (s), 1964(s). IR (cm^{-1}, Nujol mull): 613 (s), 604 (s), 575 (s), 563 (m), 498 (m). 443 (m), 409 (m), 381 (m), 333 (m).

Synthesis of $[Et_4N]_2[Fe_6(CO)_{12}Se_6]$, IVb. Method A. A Schlenk flask was charged with 0.10 g (0.25 mmol) of K_2Se_4 and 10 mL of DMF. The solution was stirred until the polyselenide was dissolved, generating a dark green-brown solution. A 0.17 mL (1.3 mmol) aliquot of $Fe(CO)_5$ was added and the mixture stirred at 100 °C for 40 min. To the golden brown solution was added 0.11 g (0.53 mmol) of Et_4NBr with stirring and the DMF removed under vacuum. Methylene chloride and ether workup as described above resulted in formation of dark purple hexagonal plates of the product in 13% yield. Anal. Calcd for $C_{28}H_{40}O_{12}N_2Fe_6Se_6$: C, 23.93; H, 2.87; N, 1.99. Found: C, 24.01; H, 3.06; N, 1.95. IR (cm^{-1}, DMF) (ν_{CO}): 2031 (s), 2003 (s), 1958(s). IR (cm^{-1} Nujol mull): 609 (s), 576 (s), 560 (s), 494 (w), 468 (w), 439 (m).

Method B. A Schlenk flask was charged with 0.10 g (0.25 mmol) of K_2Se_4 and 0.040 g (0.51 mmol) of gray Se, and 10 mL of DMF was added. The solution was stirred until the polyselenide was dissolved, generating a dark green solution. A 0.20 mL (1.5 mmol) aliquot of $Fe(CO)_5$ was added and the mixture heated in an oil bath at 100 °C for 2.5 h. To the dark brown solution was added 0.11 g (0.53 mmol) of Et_4NBr with stirring. Removal of DMF and the workup described previously provided dark purple crystals of the product in 20% yield.

Synthesis of $[Ph_4P]_2[NiFe_4(CO)_{12}S_4]\cdot CH_2Cl_2$, Va. A polysulfide solution was generated in the usual fashion by stirring 0.10 g (0.49 mmol) of K_2S_4 and 0.031 g (0.97 mmol) of elemental S in 10 mLof DMF. To the solution were added a 0.38 mL (2.9 mmol) aliquot of $Fe(CO)_5$ and 0.31 g (0.49 mmol) of $Ni(CO)_2(PPh_3)_2$, and the mixture was stirred at 23 °C for 2 days. To the resulting brown solution was added 0.41 g (0.98 mmol) of Ph_4PBr with stirring and the DMF removed under vacuum. The aforementioned workup provided dark brown needles of the product in 39% yield. Semiquantitative EDXS showed that Fe, Ni, and S were present in approximately the correct stoichiometries. Anal. Calcd for $C_{61}H_{42}O_{12}Cl_2P_2Fe_4NiS_4$: C, 48.50; H, 2.80. Found: C, 49.99; H, 3.00. IR (cm^{-1}, DMF) (ν_{CO}): 2018 (s), 1995 (s), 1941 (s). IR (cm^{-1}, Nujol mull): 614 (s), 580 (s), 567 (s), 525 (s), 454 (m), 377 (m), 196 (m).

Synthesis of $[Et_4N]_2[NiFe_4(CO)_{12}Se_4]$, Vb. A polyselenide solution was prepared by combining 0.10 g (0.25 mmol) of K_2Se_4 and 0.040 g (0.51 mmol) of gray Se in 10 mL of DMF. The solution was stirred until the polyselenide was dissolved, forming a dark green solution. A 0.20 mL (1.5 mmol) aliquot of $Fe(CO)_5$ was added and the mixture heated in an oil bath at 100 °C for 1 h. To the brown solution was added 0.16 g (0.25 mmol) of $Ni(CO)_2(PPh_3)_2$ and the mixture stirred at 100 °C for an additional 45 min. After addition of 0.11 g (0.53 mmol), Et_4NBr to the dark brown solution, workup as for **Va** yielded brown needles of the product in 23% yield. Semiquantitiative EDXS showed that Fe, Ni, and Se were present in approximately correct stoichiometries. Anal. Calcd for $C_{28}H_{40}O_{12}N_2Fe_4NiSe_4$: C, 28.14; H, 3.35; N, 2.35. Found: C, 27.90; H, 3.40; N, 2.40. IR (cm^{-1}, DMF) (ν_{CO}): 2013 (s), 1989 (s), 1935 (s). IR (cm^{-1}, Nujol mull): 612 (s), 578 (s), 566 (s), 448 (m), 286 (m).

Table 1. Crystallographic Data

	Ib	II	III	IVa	IVb	Va
formula	$C_{57}H_{40}O_9P_2Fe_3Se$	$C_{46}H_{72}N_2O_{14}S_2Fe_5$	$C_{62}H_{40}O_{14}P_2Fe_5Se_2$	$C_{28}H_{40}N_2O_{12}S_6Fe_6$	$C_{28}H_{40}N_2O_{12}Fe_6Se_6$	$C_{62}H_{44}O_{12}P_2S_4Cl_4Fe_4Ni$
fw	1177.34	1220.44	1508.09	1124.08	1405.48	1595.06
space group	$P\bar{1}$	$P2_1/c$	$P\bar{1}$	$P2_1/n$	$P2_1/c$	$P\bar{1}$
a, Å	11.580(4)	33.284(7)	12.951(4)	14.037(4)	12.134(2)	11.270(4)
b, Å	12.369(3)	18.769(4)	13.155(6)	12.053(4)	12.753(2)	12.038(5)
c, Å	19.707(4)	18.704(4)	20.729(8)	14.834(4)	16.058(2)	12.664(5)
α, deg	88.18(2)		98.01(3)			79.53(3)
β, deg	81.78(2)	90.945(5)	94.25(3)	112.51(2)	109.050(8)	82.55(3)
γ, deg	71.32(2)		115.77(3)			89.32(3)
V, Å^3	2646(1)	11683(10)	3113(2)	2318.5(9)	2348.8(5)	1675(1)
Z	2	8	2	2	2	1
ϱ_{calc}, g/cm^3	1.48	1.39	1.61	1.61	1.99	1.58
μ, mm^{-1}	1.62	1.34	2.30	2.15	6.50	1.51
transm coeff	0.93−1.00	0.83−1.00	0.71−1.00	0.41−1.00	0.80−1.00	0.81−1.00
R^a	0.0322	0.0987	0.0742	0.0421	0.0307	0.0543
$R_w{}^b$	0.0358	0.1179	0.0883	0.0569	0.0335	0.0699

^{a} $R = \sum||F_o| - |F_c||/\sum|F_o|$. ^{b} $R_w = [\sum_w(|F_o| - |F_c|)^2/\sum_w|F_o|^2]^{1/2}$; $w = 1/[\sigma^2(F_o) + gF_o^2]$.

Synthesis of $[Ph_4P]_2[PdFe_4(CO)_{12}S_4]\cdot CH_2Cl_2$, VI. This compound was prepared similarly to the Ni analog. A polysulfide solution was generated by stirring 0.050 g (0.24 mmol) of K_2S_4 and 0.015 g (0.47 mmol) of S_8 in 10 mL of DMF. A 0.19 mL (1.5 mmol) aliquot of $Fe(CO)_5$ was added to the solution, and the mixture was stirred at 23 °C for 2 h. To the resultant brown solution was added 0.28 g (0.24 mmol) of $Pd(PPh_3)_4$, along with an additional 0.031 g (0.97 mmol) of S_8. After 21 h of stirring at 23 °C, the previously described workup procedure provided red-brown needles of the product in 30% yield. Semiquantitative EDXS showed that Fe, Pd, and S were present in approximately correct stoichiometries. Anal. Calcd for $C_{61}H_{42}O_{12}Cl_2P_2Fe_4PdS_4$: C, 47.80; H, 2.70. Found: C, 47.85; H, 2.77; IR (cm^{-1}, DMF) (ν_{CO}): 2021 (s), 1997 (s), 1941 (s).

X-ray Structure Analysis. Intensity measurements were made at room temperature (21 °C) on either a Nicolet R3mV diffractometer (**Ib**, **III**−**Va**) or a refurbished (crystal Logic, Inc.) Syntex $P2_1$ diffractometer (**II**) with graphite-monochromated Mo Kα radiation (λ = 0.710 73 Å). Data for compound **Va** were obtained at −70 °C, while all others were obtained at room temperature. Relevant crystallographic data are given in Table 1. Data were measured to $2\theta = 45°$ (40° for **II**) at speeds (in ω) of 2−15°/min (6°/min for **II**; 2°/min for **III**). Periodic measurement of three standard reflections indicated crystal and electronic stability (±2%) for all compounds. Lorentz and polarization corrections and an empirical absorption correction were applied to the data for each compound.

The structures were solved by direct methods and refined by full-matrix least-squares techniques using the SHELXTL-Plus package of programs. All non-hydrogen atoms were refined anisotropically, unless described otherwise below. Hydrogen atoms were included in the structure factor calculation for each compound at optimized positions (d_{C-H} = 0.96 Å) with a refined group thermal parameter (U_H: 0.078(4) Å^2 for **Ib**; 0.08(1) Å^2 for **III**; 0.21(2) Å^2 for **IVb**; 0.06(1) Å^2 for **Va**; hydrogen atoms were not included for **II** and **IVa**). The *n*-butylammonium cations of **II** were badly disordered, but the positional and thermal parameters of the anion were not significantly affected by any of a variety of methods to model this disorder. In the final cycle of refinement, the N−C and C−C distances of the cations were constrained to equivalent values for all chemically related groups. In **IVa**, the ethyl groups of the cation were disordered over two sites: the half-occupancy carbon atoms were refined isotropically. The anions of compounds **IVa** and **IVb** are both situated about inversion centers ($^1/_2$, $^1/_2$, $^1/_2$ in both cases). The Ni atom of **Va** is located on an inversion center at the origin; the asymmetric unit also contains a methylene chloride solvent molecule.

Positional parameters of the anions are given in Tables 2−7 for compounds **Ib**−**Va**, respectively. Selected distances and angles are listed in Tables 8−13 for the six compounds.

Table 2. Atomic Coordinates (×10^4) and Equivalent Isotropic Displacement Coefficients (Å^2 × 10^3) for **Ib**

	x	y	z	$U_{eq}{}^a$
Se(1)	2152(1)	1456(1)	1858(1)	49(1)
Fe(1)	934(1)	1726(1)	2917(1)	54(1)
Fe(2)	3338(1)	837(1)	2734(1)	48(1)
Fe(3)	1987(1)	−259(1)	2293(1)	46(1)
O(1)	−1506(7)	2208(7)	2532(4)	119(4)
O(2)	757(7)	4036(6)	3289(4)	118(4)
O(3)	395(7)	854(7)	4275(3)	111(4)
O(4)	3999(6)	2861(5)	2962(3)	92(4)
O(5)	5687(6)	−685(6)	2070(4)	101(4)
O(6)	3410(7)	−84(6)	4114(3)	95(4)
O(7)	3958(6)	−1858(6)	1389(3)	91(3)
O(8)	−194(6)	−423(6)	1770(3)	86(3)
O(9)	1935(6)	−1656(5)	3512(3)	79(3)
C(1)	−505(9)	2019(8)	2685(5)	75(4)
C(2)	868(9)	3102(9)	3150(5)	79(5)
C(3)	659(8)	1168(8)	3741(5)	69(4)
C(4)	3734(8)	2050(8)	2878(4)	59(4)
C(5)	4751(8)	−69(7)	2333(5)	63(4)
C(6)	3351(8)	274(7)	3569(5)	62(4)
C(7)	3186(9)	−1227(8)	1750(4)	62(4)
C(8)	684(8)	−352(7)	1987(4)	64(4)
C(9)	1955(7)	−1074(7)	3044(4)	55(4)

^{a} Equivalent isotropic U defined as one-third of the trace of the orthogonalized U_{ij} tensor.

Reactivity

The reactions of neutral iron carbonyls with polysulfides and polyselenides were explored in some detail with particular emphasis on $Fe(CO)_5$. Our original goal was to prepare sulfur and selenium analogs to the new series of cubane-containing iron carbonyl tellurides,[5] because of their possible biological relevance. A rich chemistry has indeed been discovered, but it is substantially different from that of the tellurides and all attempts to prepare lighter analogs of dicubane compounds like $[Fe_8Te_{10}(CO)_{20}]^{2-}$ have been unsuccessful to date. It now seems questionable whether lighter analogs of these clusters exist under the conditions we are employing.

However a number of interesting compounds and reactivity patterns have begun to emerge. It appears that the most stable end product in most of the reactions is $[Fe_3(CO)_9E]^{2-}$. The oxide[7] and sulfide[8] analogs were prepared earlier, and we recently reported a high-yield synthesis of the telluride analog by methods similar to these described here.[4] This area has attracted a great deal of interest, and several convenient synthetic pathways to these various compounds have emerged from other laboratories, including the structure of the PPN^+ salt of **Ib**.[9] In

(7) Ceriotti, A.; Resconi, L.; Demartin, F.; Longoni, G.; Manassero, M.; Sabsoni, M. *J. Organomet. Chem.* **1983**, *249*, C35.
(8) Zhigui, Z.; Lixin, W.; Hengbin, Z.; Ling, Y.; Yuguo, F. *Eur. J. Solid State Inorg. Chem.* **1991**, *28*, 1269.

Table 3. Atomic Coordinates ($\times 10^4$) and Equivalent Isotropic Displacement Coefficients ($Å^2 \times 10^3$) for **II**

	x	y	z	U_{eq}[a]
Fe(1)	1171(1)	4867(2)	2400(2)	68(2)
Fe(2)	1631(1)	5825(2)	3020(2)	81(2)
Fe(3)	948(1)	5539(2)	3556(2)	76(2)
Fe(4)	1211(1)	4348(3)	1098(2)	84(2)
Fe(5)	1066(1)	3504(2)	2141(2)	81(2)
Fe(6)	3722(1)	122(2)	2178(2)	78(2)
Fe(7)	3643(1)	−137(3)	810(2)	90(2)
Fe(8)	3843(2)	−1151(3)	1651(3)	104(2)
Fe(9)	3445(1)	1243(3)	2857(3)	93(2)
Fe(10)	4132(2)	726(3)	3217(3)	93(2)
S(1)	1451(2)	4815(4)	3478(4)	77(3)
S(2)	1618(2)	4109(4)	1987(4)	78(4)
S(3)	4192(3)	−215(5)	1448(5)	95(4)
S(4)	3968(3)	1214(4)	2190(4)	85(4)
O(1)	304(7)	4774(12)	2368(12)	123(12)
O(2)	1078(9)	6148(12)	1510(12)	155(14)
O(3)	2139(9)	6228(17)	4197(16)	180(16)
O(4)	1379(8)	7252(14)	2687(14)	154(15)
O(5)	2261(8)	5618(14)	1983(14)	148(13)
O(6)	1128(8)	6301(15)	4838(13)	159(14)
O(7)	315(8)	4689(14)	4182(14)	158(14)
O(8)	460(8)	6653(13)	2929(12)	126(12)
O(9)	1702(8)	5257(13)	314(13)	148(13)
O(10)	408(9)	4776(14)	628(13)	151(14)
O(11)	1265(7)	3156(14)	177(11)	119(12)
O(12)	230(7)	3244(15)	1648(15)	158(15)
O(13)	1020(7)	3132(12)	3643(12)	111(11)
O(14)	1379(8)	2167(13)	1629(13)	146(13)
O(15)	3603(8)	−814(13)	3399(12)	152(14)
O(16)	2841(8)	37(16)	1936(13)	158(15)
O(17)	3501(6)	1329(13)	444(11)	111(11)
O(18)	4015(9)	−546(16)	−522(15)	184(17)
O(19)	2859(8)	−809(15)	466(14)	156(14)
O(20)	3048(9)	−1728(14)	1974(15)	163(15)
O(21)	4356(12)	−1888(15)	2683(16)	241(22)
O(22)	4012(9)	−2041(16)	463(15)	183(17)
O(23)	3590(9)	2460(15)	3758(16)	197(18)
O(24)	2914(8)	506(15)	3859(13)	150(14)
O(25)	2869(10)	1931(18)	1880(17)	200(19)
O(26)	4591(10)	1955(15)	3618(17)	203(18)
O(27)	4788(8)	−315(12)	3116(12)	129(12)
O(28)	3815(10)	412(20)	4647(17)	223(21)
C(1)	654(12)	4777(16)	2440(16)	83(11)
C(2)	1143(10)	5647(18)	1859(17)	89(11)
C(3)	1943(17)	6069(26)	3703(29)	175(21)
C(4)	1491(11)	6682(21)	2857(18)	98(12)
C(5)	2022(11)	5682(18)	2432(18)	97(12)
C(6)	1062(12)	6013(20)	4264(23)	118(14)
C(7)	575(11)	5008(18)	3916(17)	96(11)
C(8)	672(11)	6220(19)	3160(18)	88(12)
C(9)	1469(12)	4882(21)	655(20)	109(13)
C(10)	722(13)	4579(20)	823(20)	110(14)
C(11)	1246(11)	3630(20)	550(20)	102(14)
C(12)	540(13)	3330(19)	1829(20)	113(14)
C(13)	1055(10)	3259(17)	3060(18)	86(12)
C(14)	1249(11)	2687(19)	1832(17)	94(12)
C(15)	3661(11)	−429(19)	2932(20)	107(13)
C(16)	3180(13)	107(20)	1993(20)	115(14)
C(17)	3555(10)	741(19)	607(17)	84(11)
C(18)	3851(13)	−376(22)	43(25)	142(16)
C(19)	3152(14)	−575(21)	628(21)	121(15)
C(20)	3358(13)	−1540(21)	1833(20)	118(15)
C(21)	4140(13)	−1604(23)	2299(24)	142(16)
C(22)	3923(14)	−1652(26)	1002(27)	160(18)
C(23)	3520(12)	1995(23)	3385(22)	127(15)
C(24)	3115(12)	795(19)	3470(20)	108(14)
C(25)	3107(14)	1675(22)	2258(22)	130(16)
C(26)	4416(13)	1431(24)	3527(21)	133(16)
C(27)	4543(10)	110(17)	3144(16)	79(10)
C(28)	3927(13)	525(22)	4070(24)	130(16)

[a] Equivalent isotropic U defined as one-third of the trace of the orthogonalized $\mathbf{U}_{ij}$ tensor.

Table 4. Atomic Coordinates ($\times 10^4$) and Equivalent Isotropic Displacement Coefficients ($Å^2 \times 10^3$) for **III**

	x	y	z	U_{eq}[a]
Se(1)	4319(1)	1140(2)	7991(1)	47(1)
Se(2)	2783(2)	1240(2)	6737(1)	49(1)
Fe(1)	2417(2)	−24(2)	7476(1)	39(1)
Fe(2)	4117(2)	−623(2)	7459(1)	46(1)
Fe(3)	3412(2)	−274(2)	8572(1)	45(1)
Fe(4)	1539(2)	1448(2)	7428(1)	54(1)
Fe(5)	946(2)	−243(2)	6446(1)	50(1)
O(1)	612(10)	−725(13)	8321(6)	70(7)
O(2)	1364(12)	−2448(11)	6845(7)	71(7)
O(3)	4155(13)	−583(13)	6048(7)	82(9)
O(4)	3301(14)	−3074(13)	7444(9)	110(11)
O(5)	6545(12)	−38(13)	7822(8)	90(9)
O(6)	2780(17)	904(15)	9663(7)	106(12)
O(7)	1805(13)	−2655(12)	8547(7)	83(8)
O(8)	5437(12)	−244(13)	9310(7)	83(8)
O(9)	2867(18)	2888(18)	8696(9)	121(13)
O(10)	1340(15)	3299(14)	6900(8)	109(12)
O(11)	−845(12)	451(15)	7696(9)	103(10)
O(12)	1390(12)	−1641(12)	5377(7)	75(8)
O(13)	−1137(12)	−2018(13)	6784(8)	94(8)
O(14)	−101(15)	836(16)	5658(7)	108(12)
C(1)	1363(13)	−351(16)	8022(8)	48(8)
C(2)	1873(15)	−1480(17)	7084(8)	51(9)
C(3)	4176(17)	−560(18)	6606(9)	62(11)
C(4)	3581(16)	−2113(18)	7453(9)	60(10)
C(5)	5587(16)	−263(18)	7683(10)	70(12)
C(6)	2980(17)	398(19)	9225(10)	67(11)
C(7)	2400(16)	−1710(18)	8556(9)	57(9)
C(8)	4677(15)	−234(16)	9009(8)	55(9)
C(9)	2355(20)	2323(22)	8192(14)	87(15)
C(10)	1420(16)	2561(19)	7118(9)	66(11)
C(11)	60(21)	796(21)	7587(11)	83(15)
C(12)	1199(15)	−1100(17)	5780(9)	58(10)
C(13)	−300(16)	−1297(19)	6666(10)	68(11)
C(14)	297(18)	377(19)	5956(9)	70(12)

[a] Equivalent isotropic U defined as one-third of the trace of the orthogonalized $\mathbf{U}_{ij}$ tensor.

Table 5. Atomic Coordinates ($\times 10^4$) and Equivalent Isotropic Displacement Coefficients ($Å^2 \times 10^3$) for **IVa**

	x	y	z	U_{eq}[a]
Fe(1)	5413(1)	5498(1)	4427(1)	39(1)
Fe(2)	6454(1)	5628(1)	2925(1)	45(1)
Fe(3)	6087(1)	7484(1)	3481(1)	57(1)
S(1)	5247(1)	3700(1)	4607(1)	45(1)
S(2)	4841(1)	6136(1)	2856(1)	50(1)
S(3)	7001(1)	6116(1)	4546(1)	49(1)
O(1)	6663(4)	3208(5)	3090(4)	73(3)
O(2)	5582(5)	5898(6)	804(4)	105(3)
O(3)	8544(5)	5984(6)	3025(6)	108(4)
O(4)	8080(6)	8560(6)	3985(6)	129(4)
O(5)	5286(6)	8906(5)	4631(5)	117(4)
O(6)	5161(7)	8594(6)	1596(5)	131(5)
C(1)	6540(5)	4137(6)	3021(5)	51(3)
C(2)	5919(6)	5791(7)	1634(6)	68(4)
C(3)	7720(6)	5852(6)	3000(6)	66(3)
C(4)	7295(8)	8136(7)	3777(6)	81(4)
C(5)	5589(7)	8333(6)	4189(6)	78(4)
C(6)	5523(8)	8154(7)	2332(7)	86(5)

[a] Equivalent isotropic U defined as one-third of the trace of the orthogonalized $\mathbf{U}_{ij}$ tensor.

this paper we present simple high-yield routes to these compounds, which can be easily crystallized as a variety of quaternary -onium salts. These simple preparations provide a convenient entry into a complete series of compounds for further comparative study.

(9) (a) Shieh, M.; Tsai, Y.-C. *Inorg. Chem.* **1994**, *33*, 2303. (b) Bachman, R. E.; Whitmire, K. H. *Inorg. Chem.* **1994**, *33*, 2527.

Table 6. Atomic Coordinates ($\times 10^4$) and Equivalent Isotropic Displacement Coefficients ($Å^2 \times 10^3$) for **IVb**

	x	y	z	U_{eq}[a]
Se(1)	4827(1)	5288(1)	6093(1)	63(1)
Se(2)	3560(1)	2566(1)	4976(1)	60(1)
Se(3)	1975(1)	4637(1)	4038(1)	58(1)
Fe(1)	4025(2)	4370(1)	4785(1)	56(1)
Fe(2)	1729(2)	3296(2)	5025(1)	56(1)
Fe(3)	2029(2)	2827(2)	3572(1)	57(1)
O(1)	2442(11)	4343(9)	6751(7)	103(6)
O(2)	−697(11)	3914(9)	4442(8)	109(6)
O(3)	1105(11)	1223(9)	5488(7)	104(6)
O(4)	3320(10)	3028(8)	2335(6)	81(5)
O(5)	−318(11)	3162(11)	2340(8)	125(7)
O(6)	1775(12)	553(9)	3584(7)	107(6)
C(1)	2206(14)	3942(13)	6071(10)	80(8)
C(2)	278(15)	3671(12)	4685(10)	75(8)
C(3)	1365(14)	2047(14)	5325(9)	74(7)
C(4)	2819(14)	2947(12)	2836(9)	75(7)
C(5)	600(15)	3060(12)	2829(9)	79(8)
C(6)	1863(14)	1457(12)	3564(9)	72(7)

[a] Equivalent isotropic U defined as one-third of the trace of the orthogonalized U_{ij} tensor.

Table 7. Atomic Coordinates ($\times 10^4$) and Equivalent Isotropic Displacement Coefficients ($Å^2 \times 10^3$) for **Va**

	x	y	z	U_{eq}[a]
Ni(1)	0	0	0	20(1)
Fe(1)	842(2)	2595(1)	−506(1)	25(1)
Fe(2)	−465(2)	2071(1)	1269(1)	26(1)
S(1)	1133(3)	1016(2)	730(3)	26(1)
S(2)	−917(3)	1623(2)	−308(3)	25(1)
O(1)	2002(8)	2110(8)	−2561(8)	46(4)
O(2)	2812(9)	3625(8)	304(8)	49(4)
O(3)	−332(10)	4656(8)	−1386(10)	66(5)
O(4)	−2047(9)	542(8)	2896(8)	55(4)
O(5)	1067(10)	2887(9)	2682(8)	56(4)
O(6)	−2147(10)	3951(8)	1059(9)	62(5)
C(1)	1566(12)	2282(10)	−1744(11)	31(5)
C(2)	2048(12)	3238(10)	−35(11)	33(5)
C(3)	140(13)	3860(11)	−1046(12)	38(5)
C(4)	−1413(12)	1090(11)	2256(10)	30(5)
C(5)	429(14)	2600(12)	2130(12)	46(6)
C(6)	−1476(14)	3226(11)	1141(10)	37(5)

[a] Equivalent isotropic U defined as one-third of the trace of the orthogonalized U_{ij} tensor.

Table 8. Selected Bond Distances (Å) and Angles (deg) for **Ib**

Distances			
Se(1)−Fe(1)	2.315 (2)	Se(1)−Fe(2)	2.319 (2)
Se(1)−Fe(3)	2.317 (2)	Fe(1)−Fe(2)	2.620 (2)
Fe(1)−Fe(3)	2.621 (2)	Fe(1)−C(1)	1.714 (10)
Fe(1)−C(2)	1.753 (11)	Fe(1)−C(3)	1.771 (9)
Fe(2)−Fe(3)	2.620 (2)	Fe(2)−C(4)	1.746 (10)
Fe(2)−C(5)	1.752 (8)	Fe(2)−C(6)	1.766 (9)
Fe(3)−C(7)	1.760 (8)	Fe(3)−C(8)	1.741 (11)
Fe(3)−C(9)	1.767 (9)	O(1)−C(1)	1.188 (13)
O(2)−C(2)	1.157 (13)	O(3)−C(3)	1.144 (12)
O(4)−C(4)	1.162 (13)	O(5)−C(5)	1.167 (10)
O(6)−C(6)	1.152 (11)	O(7)−C(7)	1.149 (10)
O(8)−C(8)	1.186 (13)	O(9)−C(9)	1.154 (10)

Angles			
Fe(1)−Se(1)−Fe(2)	68.8(1)	Fe(1)−Se(1)−Fe(3)	68.9(1)
Fe(2)−Se(1)−Fe(3)	68.8(1)	Se(1)−Fe(1)−Fe(2)	55.7(1)
Se(1)−Fe(1)−Fe(3)	55.6(1)	Fe(2)−Fe(1)−Fe(3)	60.0(1)

The reaction of an excess of iron carbonyl with almost any polysulfide or -selenide will eventually lead to the formation of $[Fe_3(CO)_9(\mu_3\text{-}E)]^{2-}$.

$$Fe(CO)_5(\text{excess}) + E_n^{2-} \rightarrow [Fe_3(CO)_9(\mu_3\text{-}E)]^{2-}$$

In fact, most of the other clusters described in this paper will ultimately convert irreversibly to $[Fe_3(CO)_9(\mu_3\text{-}E)]^{2-}$ in the presence of excess iron carbonyl in solution. Thus, all other compounds in this system must be prepared from an initial mixture of equimolar or excess amounts of polychalcogenide relative to the metal carbonyl.

Table 9. Selected Bond Distances (Å) and Angles (deg) for **II**

Distances			
Fe(1)−Fe(2)	2.617(6)	Fe(1)−Fe(3)	2.621(6)
Fe(1)−Fe(4)	2.628(6)	Fe(1)−Fe(5)	2.626 (6)
Fe(1)−S(1)	2.209(8)	Fe(1)−S(2)	2.208 (9)
Fe(1)−C(1)	1.734(39)	Fe(1)−C(2)	1.781 (34)
Fe(2)−Fe(3)	2.555(6)	Fe(2)−S(1)	2.169 (9)
Fe(2)−C(3)	1.696(53)	Fe(2)−C(4)	1.702 (39)
Fe(2)−C(5)	1.740(37)	Fe(3)−S(1)	2.163 (9)
Fe(3)−C(6)	1.634(40)	Fe(3)−C(7)	1.736 (36)
Fe(3)−C(8)	1.731(35)	Fe(4)−Fe(5)	2.566 (6)
Fe(4)−S(2)	2.173(9)	Fe(4)−C(9)	1.565 (40)
Fe(4)−C(10)	1.755(42)	Fe(4)−C(11)	1.699 (38)
Fe(5)−S(2)	2.182(9)	Fe(5)−C(12)	1.865 (44)
Fe(5)−C(13)	1.779(35)	Fe(5)−C(14)	1.753 (36)
Fe(6)−Fe(7)	2.613(6)	Fe(6)−Fe(8)	2.618 (7)
Fe(6)−Fe(9)	2.632(7)	Fe(6)−Fe(10)	2.616 (6)
Fe(6)−S(3)	2.185(10)	Fe(6)−S(4)	2.207 (9)
Fe(6)−C(15)	1.763(38)	Fe(6)−C(16)	1.831 (44)
Fe(7)−Fe(8)	2.550(7)	Fe(7)−S(3)	2.172 (10)
Fe(7)−C(17)	1.716(36)	Fe(7)−C(18)	1.666 (47)
Fe(7)−C(19)	1.854(45)	Fe(8)−S(3)	2.144 (10)
Fe(8)−C(20)	1.809(44)	Fe(8)−C(21)	1.768 (44)
Fe(8)−C(22)	1.563(51)	Fe(9)−Fe(10)	2.564 (7)
Fe(9)−S(4)	2.159(10)	Fe(9)−C(23)	1.739 (43)
Fe(9)−C(24)	1.807(39)	Fe(9)−C(25)	1.773 (44)
Fe(10)−S(4)	2.189(9)	Fe(10)−C(26)	1.721 (44)
Fe(10)−C(27)	1.798(34)	Fe(10)−C(28)	1.785 (44)

Angles			
Fe(2)−Fe(1)−Fe(3)	58.4(2)	Fe(2)−Fe(1)−Fe(4)	128.8(2)
Fe(3)−Fe(1)−Fe(4)	164.1(2)	Fe(2)−Fe(1)−Fe(5)	145.6(2)
Fe(3)−Fe(1)−Fe(5)	125.6(2)	Fe(4)−Fe(1)−Fe(5)	58.5(2)
Fe(2)−Fe(1)−S(1)	52.6(2)	Fe(3)−Fe(1)−S(1)	52.4(2)
Fe(4)−Fe(1)−S(1)	143.4(3)	Fe(5)−Fe(1)−S(1)	100.2(3)
Fe(2)−Fe(1)−S(2)	101.9(3)	Fe(3)−Fe(1)−S(2)	143.3(3)
Fe(4)−Fe(1)−S(2)	52.5(2)	Fe(5)−Fe(1)−S(2)	52.8(2)
S(1)−Fe(1)−S(2)	90.9(3)	Fe(1)−Fe(2)−S(1)	54.0(2)
Fe(1)−Fe(2)−Fe(3)	60.9(2)	Fe(1)−Fe(3)−S(1)	54.0(2)
Fe(3)−Fe(2)−S(1)	53.8(3)	Fe(1)−Fe(3)−Fe(2)	60.7(2)
Fe(1)−Fe(4)−Fe(5)	60.7(2)	Fe(1)−Fe(4)−S(2)	53.7(2)
Fe(5)−Fe(4)−S(2)	54.1(3)	Fe(1)−Fe(5)−S(2)	53.7(2)
Fe(1)−Fe(5)−Fe(4)	60.8(2)	Fe(7)−Fe(6)−C(15)	131.5(12)
Fe(4)−Fe(5)−S(2)	53.8(2)	Fe(2)−Fe(3)−S(1)	54.0(3)
Fe(7)−Fe(6)−Fe(8)	58.4(2)	Fe(7)−Fe(6)−Fe(9)	126.2(2)
Fe(8)−Fe(6)−Fe(9)	165.5(2)	Fe(7)−Fe(6)−Fe(10)	148.4(2)
Fe(8)−Fe(6)−Fe(10)	126.5(2)	Fe(9)−Fe(6)−Fe(10)	58.5(2)
Fe(7)−Fe(6)−S(3)	52.9(3)	Fe(8)−Fe(6)−S(3)	52.1(3)
Fe(9)−Fe(6)−S(3)	142.4(3)	Fe(10)−Fe(6)−S(3)	102.7(3)
Fe(7)−Fe(6)−S(4)	102.4(3)	Fe(8)−Fe(6)−S(4)	142.4(3)
Fe(9)−Fe(6)−S(4)	52.1(3)	Fe(10)−Fe(6)−S(4)	53.2(3)
S(3)−Fe(6)−S(4)	90.3(4)		

The bright red crystals of the $[Fe_3(CO)_9(\mu_3\text{-}E)]^{2-}$ salts are occasionally contaminated with small amounts of darker red−brown crystals, which on further examination prove to be $[Fe_5(CO)_{14}(\mu_3\text{-}E)_2]^{2-}$ (E = S, Se). These compounds were subsequently synthesized in reasonable yields by the reaction of E_2^{2-} with excess iron carbonyl.

$$E_2^{2-} + 5Fe(CO)_5 \rightarrow [Fe_5(CO)_{14}(\mu_3\text{-}E)_2]^{2-}$$

Under these reaction conditions, this cluster can usually be isolated cleanly in reasonable yields. For reasons which are not clear, the sulfide does not crystallize well as its PPh_4^+ salt but crystallizes quite well as the n-Bu_4N^+ salt. The length of the polychalcogenide chain and the relative ratios were further varied over a wide range, and they invariably led to mixtures of $[Fe_5(CO)_{14}(\mu_3\text{-}E)_2]^{2-}$ and $[Fe_3(CO)_9(\mu_3\text{-}E)]^{2-}$, or $[Fe_5(CO)_{14}(\mu_3$-

Table 10. Selected Bond Distances (Å) and Angles (deg) for **III**

Distances			
Se(1)−Fe(1)	2.329(3)	Se(1)−Fe(2)	2.320(4)
Se(1)−Fe(3)	2.285(3)	Se(2)−Fe(1)	2.340(3)
Se(2)−Fe(4)	2.311(4)	Se(2)−Fe(5)	2.293(3)
Fe(1)−Fe(2)	2.643(4)	Fe(1)−Fe(3)	2.658(4)
Fe(1)−Fe(4)	2.646(5)	Fe(1)−Fe(5)	2.650(4)
Fe(1)−C(1)	1.784(17)	Fe(1)−C(2)	1.770(20)
Fe(2)−Fe(3)	2.597(4)	Fe(2)−C(3)	1.789(20)
Fe(2)−C(4)	1.769(23)	Fe(2)−C(5)	1.756(21)
Fe(3)−C(6)	1.771(23)	Fe(3)−C(7)	1.764(19)
Fe(3)−C(8)	1.790(21)	Fe(4)−Fe(5)	2.589(4)
Fe(4)−C(9)	1.771(24)	Fe(4)−C(10)	1.739(27)
Fe(4)−C(11)	1.805(25)	Fe(5)−C(12)	1.800(22)
Fe(5)−C(13)	1.752(19)	Fe(5)−C(14)	1.763(27)
O(1)−C(1)	1.154(21)	O(2)−C(2)	1.162(22)
O(3)−C(3)	1.151(24)	O(4)−C(4)	1.151(29)
O(5)−C(5)	1.147(26)	O(6)−C(6)	1.163(30)
O(7)−C(7)	1.139(24)	O(8)−C(8)	1.132(27)
O(9)−C(9)	1.155(30)	O(10)−C(10)	1.167(34)
O(11)−C(11)	1.112(30)	O(12)−C(12)	1.131(27)
O(13)−C(13)	1.160(23)	O(14)−C(14)	1.157(35)

Angles			
Fe(1)−Se(1)−Fe(2)	69.3(1)	Fe(1)−Se(1)−Fe(3)	70.3(1)
Fe(2)−Se(1)−Fe(3)	68.7(1)	Fe(1)−Se(2)−Fe(4)	69.3(1)
Fe(1)−Se(2)−Fe(5)	69.8(1)	Fe(4)−Se(2)−Fe(5)	68.4(1)
Se(1)−Fe(1)−Se(2)	86.8(1)	Se(1)−Fe(1)−Fe(2)	55.2(1)
Se(2)−Fe(1)−Fe(2)	104.5(1)	Se(1)−Fe(1)−Fe(3)	54.0(1)
Se(2)−Fe(1)−Fe(3)	140.7(1)	Fe(2)−Fe(1)−Fe(3)	58.7(1)
Se(1)−Fe(1)−Fe(4)	103.3(1)	Se(2)−Fe(1)−Fe(4)	54.8(1)
Fe(2)−Fe(1)−Fe(4)	153.5(1)	Fe(3)−Fe(1)−Fe(4)	124.6(1)
Se(1)−Fe(1)−Fe(5)	141.0(1)	Se(2)−Fe(1)−Fe(5)	54.3(1)
Fe(2)−Fe(1)−Fe(5)	126.4(1)	Fe(3)−Fe(1)−Fe(5)	164.9(1)
Fe(4)−Fe(1)−Fe(5)	58.5(1)	Se(1)−Fe(1)−C(1)	114.4(5)
Se(2)−Fe(1)−C(1)	128.1(7)	Fe(2)−Fe(1)−C(1)	126.9(7)
Fe(3)−Fe(1)−C(1)	74.0(6)	Fe(4)−Fe(1)−C(1)	73.8(7)
Fe(5)−Fe(1)−C(1)	94.4(6)	Se(1)−Fe(1)−C(2)	124.8(7)
Se(2)−Fe(1)−C(2)	113.3(6)	Fe(2)−Fe(1)−C(2)	69.8(7)
Se(1)−Fe(3)−Fe(2)	56.3(1)	Fe(1)−Fe(3)−Fe(2)	60.4(1)
Se(1)−Fe(2)−Fe(3)	55.0(1)	Se(1)−Fe(2)−Fe(3)	55.0(1)
Fe(1)−Fe(2)−Fe(3)	61.0(1)	Se(1)−Fe(3)−Fe(1)	55.6(1)
Fe(1)−Fe(3)−Fe(2)	60.4(1)	Se(1)−Fe(2)−C(3)	107.4(8)

Table 11. Selected Bond Distances (Å) and Angles (deg) for **IVa**

Distances			
Fe(1)−S(1)	2.207(2)	Fe(1)−S(2)	2.288(2)
Fe(1)−S(3)	2.292(2)	Fe(1)−Fe(1a)	2.681(2)
Fe(1)−S(1a)	2.205(2)	Fe(2)−Fe(3)	2.504(2)
Fe(2)−S(2)	2.309(2)	Fe(2)−S(3)	2.303(2)
Fe(2)−C(1)	1.804(8)	Fe(2)−C(2)	1.780(8)
Fe(2)−C(3)	1.759(9)	Fe(3)−S(2)	2.306(2)
Fe(3)−S(3)	2.305(2)	Fe(3)−C(4)	1.764(11)
Fe(3)−C(5)	1.790(10)	Fe(3)−C(6)	1.775(9)
O(1)−C(1)	1.131(9)	O(2)−C(2)	1.145(10)
O(3)−C(3)	1.154(11)	O(4)−C(4)	1.145(13)
O(5)−C(5)	1.140(13)	O(6)−C(6)	1.142(11)

Angles			
S(1)−Fe(1)−S(2)	116.2(1)	S(1)−Fe(1)−S(3)	117.0(1)
S(2)−Fe(1)−S(3)	85.5(1)	S(1)−Fe(1)−Fe(1a)	52.5(1)
S(2)−Fe(1)−Fe(1a)	136.7(1)	S(3)−Fe(1)−Fe(1a)	137.8(1)
S(1)−Fe(1)−S(1a)	105.2(1)	S(2)−Fe(1)−S(1a)	116.3(1)
S(3)−Fe(1)−S(1a)	116.5(1)	Fe(3)−Fe(2)−S(2)	57.1(1)
Fe(3)−Fe(2)−S(3)	57.1(1)	S(2)−Fe(2)−S(3)	84.7(1)
Fe(3)−Fe(2)−C(1)	151.7(3)	S(2)−Fe(2)−C(1)	107.6(2)
Fe(1)−S(2)−Fe(2)	84.8(1)	Fe(1)−S(2)−Fe(3)	84.9(1)
Fe(2)−S(2)−Fe(3)	65.7(1)	Fe(1)−S(3)−Fe(2)	84.9(1)
Fe(1)−S(3)−Fe(3)	84.8(1)	Fe(2)−S(3)−Fe(3)	65.9(1)

[a] Atoms labeled with a lower-case "a" are generated by the following symmetry: $1 - x, 1 - y, 1 - z$.

$E)_2]^{2-}$ and $[Fe_6(CO)_{12}(E)_6]^{2-}$ (vide infra). It should be pointed out that there has been no previous evidence for the formation of the tellurium analog $[Fe_5(CO)_{14}(\mu_3\text{-Te})_2]^{2-}$ in our hands.[4,5]

When E_4^{2-} is reacted with elemental chalcogen and $Fe(CO)_5$, the larger $[Fe_6(CO)_{12}E_6]^{2-}$ cluster can be isolated in reasonable

Table 12. Selected Bond Distances (Å) and Angles (deg) for **IVb**[a]

Distances			
Se(1)−Fe(1)	2.324(2)	Se(1)−Fe(1a)	2.324(3)
Se(2)−Fe(1)	2.412(2)	Se(2)−Fe(2)	2.434(3)
Se(2)−Fe(3)	2.431(2)	Se(3)−Fe(1)	2.407(2)
Se(3)−Fe(2)	2.416(3)	Se(3)−Fe(3)	2.434(2)
Fe(1)−Fe(1a)	2.755(4)	Fe(2)−Fe(3)	2.548(3)
Fe(2)−C(1)	1.789(15)	Fe(2)−C(2)	1.731(18)
Fe(2)−C(3)	1.761(18)	Fe(3)−C(4)	1.755(19)
Fe(3)−C(5)	1.780(15)	Fe(3)−C(6)	1.757(16)
O(1)−C(1)	1.155(19)	O(2)−C(2)	1.161(21)
O(3)−C(3)	1.152(21)	O(4)−C(4)	1.161(22)
O(5)−C(5)	1.142(19)	O(6)−C(6)	1.160(19)

Angles			
Fe(1)−Se(1)−Fe(1a)	72.7(1)	Fe(1)−Se(2)−Fe(2)	83.9(1)
Fe(1)−Se(2)−Fe(3)	83.8(1)	Fe(2)−Se(2)−Fe(3)	63.2(1)
Fe(1)−Se(3)−Fe(2)	84.4(1)	Fe(1)−Se(3)−Fe(3)	83.8(1)
Fe(2)−Se(3)−Fe(3)	63.4(1)	Se(1)−Fe(1)−Se(2)	114.3(1)
Se(1)−Fe(1)−Se(3)	116.1(1)	Se(2)−Fe(1)−Se(3)	87.2(1)
Se(1)−Fe(1)−Se(1a)	107.3(1)	Se(2)−Fe(1)−Se(1a)	117.8(1)
Se(3)−Fe(1)−Se(1a)	113.4(1)	Se(1)−Fe(1)−Fe(1a)	53.6(1)
Se(2)−Fe(1)−Fe(1a)	137.8(1)	Se(3)−Fe(1)−Fe(1a)	134.9(1)
Se(2)−Fe(2)−Se(3)	86.5(1)	Se(2)−Fe(2)−Fe(3)	58.4(1)
Se(3)−Fe(2)−Fe(3)	58.7(1)	Se(2)−Fe(2)−C(1)	100.8(6)

[a] Atoms labeled with a lower-case "a" are generated by the following symmetry: $1 - x, 1 - y, 1 - z$.

Table 13. Selected Bond Distances (Å) and Angles (deg) for **Va**[a]

Distances			
Ni(1)−S(1)	2.176(4)	Ni(1)−S(2)	2.194(3)
Fe(1)−Fe(2)	2.503(3)	Fe(1)−S(1)	2.282(3)
Fe(1)−S(2)	2.277(4)	Fe(1)−C(1)	1.773(14)
Fe(1)−C(2)	1.789(15)	Fe(1)−C(3)	1.774(13)
Fe(2)−S(1)	2.294(4)	Fe(2)−S(2)	2.279(4)
Fe(2)−C(4)	1.802(12)	Fe(2)−C(5)	1.778(17)
Fe(2)−C(6)	1.785(14)	O(1)−C(1)	1.139(17)
O(2)−C(2)	1.150(18)	O(3)−C(3)	1.133(17)
O(4)−C(4)	1.126(15)	O(5)−C(5)	1.162(20)
O(6)−C(6)	1.148(18)		

Angles			
S(1)-Ni(1)-S(2)	80.6(1)	S(1)-Ni(1)-S(2a)	99.4(1)
Fe(2)-Fe(1)-S(1)	57.1(1)	Fe(2)-Fe(1)-S(2)	56.7(1)
S(1)-Fe(1)-S(2)	76.7(1)	Fe(2)-Fe(1)-C(1)	152.1(4)
S(1)-Fe(1)-C(1)	103.7(4)	Ni(1)-S(1)-Fe(2)	91.6(1)
Fe(2)-Fe(1)-C(2)	98.3(4)	Ni(1)-S(2)-Fe(1)	91.5(1)
S(2)-Fe(1)-C(2)	154.8(4)	Fe(1)-S(2)-Fe(2)	66.7(1)
Fe(1)-S(1)-Fe(2)	66.3(1)	S(1)-Fe(1)-C(3)	156.8(5)
Ni(1)-S(2)-Fe(2)	91.5(1)	C(1)-Fe(1)-C(3)	97.8(6)
C(2)-Fe(1)-C(3)	97.2(6)	Fe(1)-Fe(2)-S(1)	56.6(1)
Fe(1)-Fe(2)-S(2)	56.6(1)	S(1)-Fe(2)-S(2)	76.4(1)
Fe(1)-Fe(2)-C(4)	152.0(4)	S(1)-Fe(2)-C(4)	104.6(4)
Ni(1)-S(1)-Fe(1)	91.8(1)	Fe(1)-Fe(2)-C(5)	99.9(5)

[a] Atoms labeled with a lower-case "a" are generated by the following symmetry: $-x, -y, -z$.

yield.

$$5Fe(CO)_5 + E_4^{2-} + 2E \rightarrow [Fe_6(CO)_{12}E_6]^{2-}$$

$$E = S, Se$$

If the elemental chalcogen is not present, then only mixtures of $[Fe_5(CO)_{14}(\mu_3\text{-}E)_2]^{2-}$ and $[Fe_3(CO)_9(\mu_3\text{-}E)]^{2-}$ are observed in solution via IR. As the ratio of elemental chalcogenide to $Fe(CO)_5$ is increased, CO stretching bands due of $[Fe_6(CO)_{12}E_6]^{2-}$ increase in intensity in the IR until it is eventually the major product in solution.

It appears that the key factor in determining the product in these reactions is the degree of reduction of the polychalcogenide starting material. If the polychalcogenide is viewed as an oxidant, then the longer the dianionic chain, the better its oxidizing ability. Thus we see that reaction of iron carbonyl

with E^{2-} leads to formation of $[Fe_3(CO)_9(\mu_3\text{-}E)]^{2-}$, a cluster in which none of the iron atoms have been oxidized. However, use of E_2^{2-} with an E–E bond leads to a more condensed (hence oxidized) cluster, $[Fe_5(CO)_{14}(\mu_3\text{-}E)_2]^{2-}$, while a very chalcogen-rich mixture (E_n^{2-} with $n > 4$) leads to formation of $[Fe_6(CO)_{12}E_6]^{2-}$, containing two formal Fe(III) centers. As with the tellurides, the more E–E bonds present in the starting material, the greater the formal oxidation states of the metal centers in the product. If it is assumed that all CO ligands are neutral and that all chalcogenides are formally 2–, then the average formal oxidation state of Fe increases from 0 for $[Fe_3(CO)_9(\mu_3\text{-}E)]^{2-}$ to +0.4 for $[Fe_5(CO)_{14}(\mu_3\text{-}E)_2]^{2-}$ to +1.67 for $[Fe_6(CO)_{12}(\mu_2\text{-}E)_6]^{2-}$. Thus we were quite eager to continue to increase the ratio of sulfur to Fe in the reaction mixture since the oxidation state of Fe in $[Fe_8Te_{10}]^{2-}$ would be 2+ (due to the presence of a ditelluride). However, we were never able to increase the polychalcogenide ratio beyond those given here. Any reaction not containing a substantial excess of $Fe(CO)_5$ resulted in rapid decomposition with immediate formation of gray insoluble amorphous powders.

It is well-known that multinuclear sulfide-bridged iron clusters will react with other metal centers by folding up to form new heterocubanes.[10] We felt that compounds like **IVa** and **IVb** might also react with metal complexes to form a new class of heterocubanes. Instead it was observed that zerovalent complexes of Ni and Pd become oxidized to a formal M(II) state. This leads to complexes which contain two $[Fe_2(CO)_6E_2]^{2-}$ groups chelating to a divalent heterometal ion, in a square planar coordination environment.

$$[Fe_6(CO)_{12}E_6]^{2-} + ML_4 \rightarrow [M\,Fe_4(CO)_{12}E_4]^{2-}$$

$$E = S, Se;\ M = Ni, Pd;\ L = CO, PPh_3$$

We have structurally characterized the molecule with iron sulfide butterflies complexed to Ni(II), but the other combinations also react cleanly, and their products have been well characterized. In general, the reaction is most facile if the iron clusters, **IVa** and **IVb**, are not isolated but prepared and used in situ. They reacted similarly if premade, but the reaction is much faster if some extra sulfur is added, presumably to complex any dissociated phosphines.

The use of $[Fe_2(CO)_6S_2]^{2-}$ units as building blocks for heterometal clusters has been previously advanced by Averill, and this concept has led to a number of fascinating new compounds.[11] However, these workers observe that complicated redox transformations can occur, leading to very complex and unusual clusters.[12] The reactions observed here are generally quite straightforward and proceed in good yield, suggesting that the iron compounds may be used as reagents for butterfly transfer to a number of different metal sites. This work is in progress.

Structures

Structure of $[Ph_4P]_2[Fe_3(CO)_9(\mu_3\text{-Se}]$, Ib. The structure of $[Ph_4P]_2[Fe_3(CO)_9(\mu_3\text{-Se})]$ contains a pyramidal structure with a triangular Fe_3 framework capped by a selenide atom (Figure 1). The Fe–Fe distances average 2.621(2) Å and are clearly within bonding distance. The Fe–Se distances average 2.317(2) and are typical of Fe–Se bonds. The carbonyl ligands are all linear and terminal and complete the six-coordinate environment surrounding the iron centers. The structure of the selenide anion with a different counterion was reported recently.[9b] It contains slightly longer Fe–Se distances with slightly shorter Fe–Fe distances but is otherwise very similar.

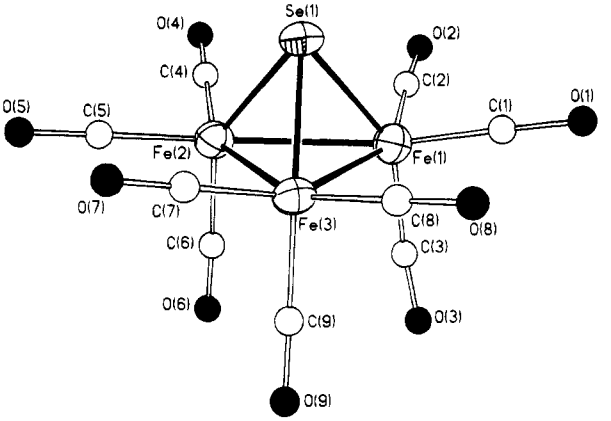

Figure 1. Thermal ellipsoid plot of the anion $[Fe_3(CO)_9(\mu_3\text{-Se}]^{2-}$, **Ib**, with ellipsoids at the 35% level.

The complete structural study for the series $[Fe_3(CO)_9(\mu_3\text{-}E)]^{2-}$ (E = O, S, Se, Te) makes it one of the few series of clusters where structures have been obtained for all members of a group. It can be observed that the Fe–Fe distances increase, as expected, when the capping group increases in size from O to Te, but the size of the increase gets progressively smaller. The average metal–metal distances range from 2.484 to 2.593 to 2.621 to 2.625 Å for O, S, Se, and Te, respectively. Note that the difference between Se and Te is almost negligible, suggesting that size of the capping element has an effect only up to a certain point, beyond which the metal–metal bond will not expand. Of course the average iron–chalcogenide distance is much more sensitive, expanding from 2.196 to 2.317 to 2.497 Å for S, Se, and Te, respectively. This leads us to postulate that for the very heavy elements the additional size is reflected mostly in the metal–element bond rather than continued expansion of a metal–metal bond.

Structure of $[n\text{-}Bu_4N]_2[Fe_5(CO)_{14}(\mu_3\text{-}S)_2]$, II. The structure of **II** consists of a well-separated anion of $[Fe_5(CO)_{14}(\mu_3\text{-}S)_2]^{2-}$ and two $[n\text{-}Bu_4N]^+$ counterions. The Ph_4P^+ salt can be formed but grows only poor crystals in low yields. There are two clusters per asymmetric unit, but while the distances and angles vary slightly, there is no substantive difference between the two clusters. The dianion contains two vertex-fused tetrahedra oriented such that the capping sulfide vertices of each tetrahedron are rotated slightly (Figure 2). The overall cluster shape is isoelectronic and nearly isostructural with an osmium dihydride complex, $H_2Os_5S_2(CO)_{14}$, prepared some years ago.[13]

The Fe–Fe bonds to the central iron atoms (average 2.623(6) Å) are longer than the Fe–Fe bonds on the edge of the cluster by about 0.06 Å. This differs from the case of $H_2Os_5S_2(CO)_{14}$, but the osmium cluster contains hydrides bridging the outer metal edges, which leads to substantial lengthening of metal–metal bonds. The central Fe–Fe bonds are slightly longer than those observed in the parent $[Fe_3(CO)_9S]^{2-}$ as well. In addition, the Fe–S bonds are slightly longer to the central iron versus the outer iron atoms (2.209(9) and 2.172(9) Å,

(10) (a) Coucouvanis, D.; Al-Ahmad, S. A.; Salifoglou, A.; Dunham, R. W.; Sands, R. H. *Angew. Chem., Int. Ed. Engl.* **1988**, *27*, 1353. (b) Coucouvanis, D.; Al-Ahmad, S. A.; Salifoglou, A.; Papaefthymiou, V.; Kostikas, A.; Simopoulos, A. *J. Am. Chem. Soc.* **1992**, *114*, 2472. (c) Roth, E. K. H.; Greneche, J. M.; Jordanov, J. *J. Chem. Soc., Chem. Commun.* **1991**, 105. (d) Ciurli, S.; Yu, S.; Holm, R. H.; Srivastava, K. K. P.; Munck, E. *J. Am. Chem. Soc.* **1990**, *112*, 8169.

(11) (a) Bose, K. S.; Lamberty, P. E.; Kovacs, J. A.; Sinn, E.; Averill, B. A. *Polyhedron* **1986**, *5*, 393. (b) Eldridge, P. A.; Bryan, R. F.; Sinn, E.; Averill, B. A. *J. Am. Chem. Soc.* **1988**, *110*, 5573. (c) Bose, K. S.; Chmielewski, S. A.; Eldridge, P. A.; Sinn, E.; Averill, B. A. *J. Am. Chem. Soc.* **1989**, *111*, 8953.

(12) Eldridge, P. A.; Bose, K. A.; Barber, D. E.; Bryan, R. F.; Sinn, E.; Rheingold, A.; Averill, B. A. *Inorg. Chem.* **1991**, *30*, 2365.

(13) Adams, R. D.; Horvàth, I. T.; Yang, L.-W. *Organometallics* **1983**, *2*, 1257.

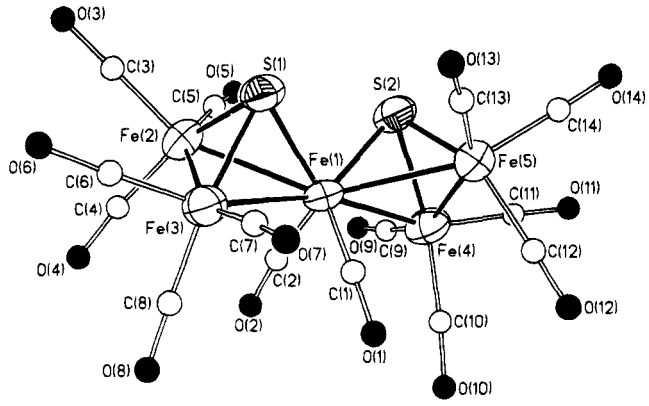

Figure 2. Thermal ellipsoid plot of the anion $[Fe_5(CO)_{14}(\mu_3\text{-}S)_2]^{2-}$, **II**, with ellipsoids at the 35% level.

respectively). All other distances and angles are unremarkable. The dihedral angles between the triiron planes average 128.5°, so the sulfide-capped vertices are rotated about 52° relative to each other. By comparison, the twist is 56.3° in the osmium cluster.

Structure of $[Ph_4P]_2[Fe_5(CO)_{14}(\mu_3\text{-}Se)_2]$, III. The structure of **III** also consists of well-separated organic counterions and two corner-shared tetrahedra with a central iron atom and face-capped selenides. In contrast to the sulfide analog, very good quality crystals of the $[Ph_4P]^+$ salt can be obtained easily. The overall $[Fe_5(CO)_{14}(\mu_3\text{-}Se)_2]^{2-}$ cluster framework is nearly identical with that of the sulfide, **II**. The Fe−Fe bonds involving the central atom are slightly elongated relative to the sulfide, as expected, to accommodate the larger capping selenide. In addition the central Fe−Se bonds are also slightly elongated but very typical for iron selenides. The twist of the two tetrahedra is 44°, which is somewhat less than in $[Fe_5(CO)_{14}(\mu_3\text{-}S)_2]^{2-}$ and the related osmium analog.

Structure of $[Et_4N]_2[Fe_6(CO)_{12}E_6$, (E = S, Se), IVa and IVb. Crystal structures have been determined for tetraethylammonim salts of both the sulfide and selenide analogs of this cluster. Both dianions have the same basic framework although, surprisingly, they crystallize in different unit cells.[14] It should also be noted that the sulfide anion of **IVa** was structurally characterized previously as its $[BzEt_2MeN]^+$ salt[15] and has the same essential structural features as those described here for both the sulfide and the selenide. However, the structure is reported for completeness.

The salt consists of two well-separated cations and the dianionic cluster. The molecule consists of a rhombic planar Fe_2Se_2 core which has both iron vertices chelated by $Fe_2(CO)_6Se_2$ butterflies (Figure 3). The Fe−Fe axes of the butterflies are perpendicular to the plane of the core, creating a pseudo-tetrahedral coordination environment around the core Fe atoms. The Fe−Fe distance in the butterflies are 2.545(3) Å, which is only slightly shorter than that in the parent neutral $Fe_2(CO)_6Se_2$.[16] The Fe···Fe distance across the central rhombus is somewhat longer at 2.755(4) Å and is also slightly shorter than the distance in $Fe_2Se_{12}^{2-}$, which also contains a similar Fe_2Se_2 rhomb. The trans-ring distance is substantially longer than in

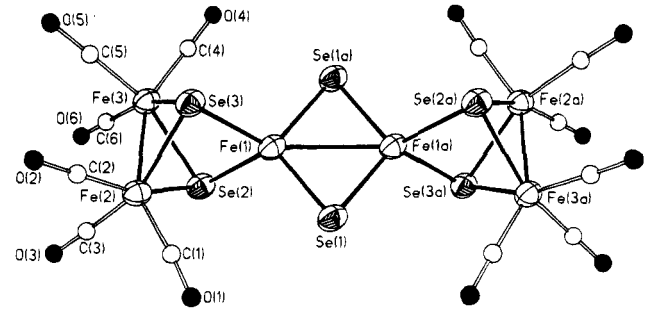

Figure 3. Thermal ellipsoid plot of the anion $[Fe_6(CO)_{12}Se_6]^{2-}$, **IVb**, with ellipsoids at the 35% level.

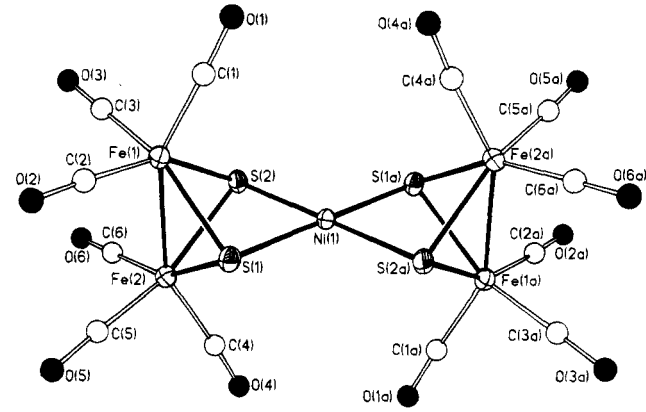

Figure 4. Thermal ellipsoid plot of the anion $[\{Fe_2(CO)_6(\mu_3\text{-}S)_2\}_2Ni]^{2-}$, **Va**, with ellipsoids at the 35% level.

the corresponding sulfides (2.693(1) Å) which can be attributed to the difference in size between bridging S and Se. The Fe−Se distances range from 2.323(3) to 2.433(3) Å, with the distances in the rhombus being the shortest followed by those bridging from the butterfly to the rhomboidal irons, while the distances within the chelating butterflies are the longest. This trend is also observed in the sulfide analog[15] and can be attributed to the increased attraction of the chalcogenide to the higher oxidation state metal centers. The carbonyl ligands have no other unusual structural features.

Structure of $[Ph_4P]_2[\{Fe_2(CO)_6(\mu_3\text{-}S)_2\}_2Ni]\cdot CH_2Cl_2$, Va. The title compound could be isolated as its tetraphenylphosphonium salt. The structure of the dianion consists of a distorted square planar nickel center chelated by two $Fe_2(CO)_6S_2$ butterflies (Figure 4). The formal oxidation states can be assigned as Ni(II) and two $[Fe_2(CO)_6S_2]^{2-}$ groups. The coordination environment around the Ni(II) center is planar, and the transannular S atoms are linear, but the two butterflies are bent by about 8° with respect to each other. The Fe−Fe bonds in the butterflies are 2.503(3) Å, a value typical of chelated dianions, but are somewhat shorter than those in the parent complex (2.552(2) Å).[17] Averill and co-workers have observed a lengthening of the Fe−Fe distance in some coordinated butterflies but have attributed this to an unusually long interaction of one of the Fe atoms with the heterometal core. The Fe−S distances in **Va** average 2.283(4) Å, which is substantially longer than the distances in the neutral parent $Fe_2(CO)_6S_2$, but this is typical of coordinated butterflies. The Ni−S distances average 2.186(4) Å, which is only slightly longer than the Ni−S distances in typical Ni(II) 1,2-dithiolenes (e.g. 2.166(6) Å in $[Ni(S_2C_2(CN)_2)_2]^{2-}$).[18] It should be noted that, in square planar Ni 1,2-dithiolenes, the Ni−S distances are very sensitive to the oxidation state of the central metal atom,[19] with Ni(IV)

(14) We performed a complete structural determination of $[(C_2H_5)_4N]_2[Fe_6(CO)_{12}(\mu\text{-}S)_6]$. Although the sulfide and selenide analogs crystallize in different space groups, the structures of the anionic clusters are completely analogous, and the sulfide is virtually identical to that previously reported of another salt.[15] Thus the structure of the sulfide is not discussed in detail, but the full solution is given in the supplementary material.

(15) Lilley, G.; Sinn, E.; Averill, B. A. *Inorg. Chem.* **1986**, *25*, 1073.

(16) Campana, C. F.; Lo, F. Y.-K.; Dahl, L. F. *Inorg. Chem.* **1979**, *18*, 3060.

(17) Wei, C. H.; Dahl, L. F. *Inorg. Chem.* **1965**, *4*, 1.

(18) Eisenberg, R.; Ibers, J. A. *Inorg. Chem.* **1965**, *4*, 605.

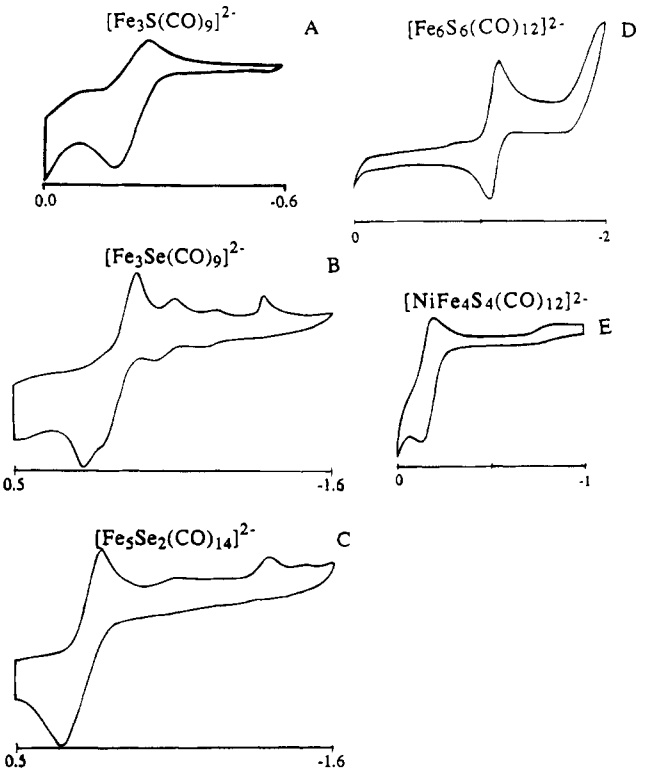

Figure 5. Cyclic voltammograms of iron chalcogenide clusters as labeled. All measurements were performed in acetonitrile at 25 °C vs SCE.

complexes having distances of ca. 2.10 Å.[20] The fact the Ni−S distances in **Va** are only slightly longer than those of metal dithiolenes suggests that the assignment of a formal Ni(II) state to the central atom in **Va** is not far afield.

It may be useful to postulate that the $[Fe_2(CO)_6S_2]^{2-}$ fragments are structural analogs of dithiolenes. They form square planar analogs of divalent metals such as Ni(II) and Pd(II) with similar structural and electronic properties (vide infra). The M−S distances are very similar to those of the metal dithiolenes, but perhaps more important are the nonbonded, trans wing tip S···S distances in the coordinated $[Fe_2S(CO)_6]^{2-}$ butterflies, since this is a measure of the bite angle. In **Va**, the square planar Ni(II) complex, the nonbonded S···S distances are 2.828(7) Å, similar to but somewhat shorter than those in square planar Ni(II) dithiolene complexes (ca. 3.00 Å). In contrast, the trans-wing S···S distances in **IVa**, which is a tetrahedral Fe(III) complex, are slightly longer at 3.108(5) Å. This structural flexibility suggests that the $[Fe_2S(CO)_6]^{2-}$ ligand might be a useful structural analog of the dithiolenes.

Electrochemistry

The redox properties of several of these clusters were probed using electrochemistry. Cyclic voltammograms of the complexes obtained in acetonitrile at ambient temperature are shown in Figure 5. The redox potentials are listed in Table 14 and are measured relative to SCE. All of the compounds undergo a sequence of irreversible multielectron oxidations at potentials greater than 0.10 V. These are probably oxidative decomposition of the structures and were not investigated further. However, each complex displays reversible reduction waves which are in the range observed for a number of iron carbonyl sulfides and selenides.[11,15,21]

Table 14. Cyclic Voltammetric Data for Iron Carbonyl Complexes[a]

complex	$E_{1/2}$, V (ΔE, mV)[b]
$[Ph_4P]_2[Fe_3(CO)_{12}S]$ (**Ia**)	−0.21 (80)
$[Ph_4P]_2[Fe_3(CO)_{12}Se]$ (**Ib**)	−0.20 (220)
	−0.51 (115)
	−0.81 (60)
$[n\text{-}Bu_4N]_2[Fe(CO)_{14}S_2]$ (**II**)	+0.016 (93)
	−1.60 (130)
$[Ph_4P]_2[Fe(CO)_{14}Se_2]$ (**III**)	+0.06 (250)
$[Et_4N]_2[Fe_6(CO)_{12}S_6]$ (**IVa**)	−1.083 (85)
$[Et_4N]_2[Fe_6(CO)_{12}Se_6]$ (**IVb**)	−1.01 (60)
$[Ph_4P]_2[NiFe_4(CO)_{12}S_4]$ (**Va**)	−0.0225 (70)
$[Ph_4P]_2[NiFe_4(CO)_{12}Se_4]$ (**Vb**)	−0.203 (275)
$[Ph_4P]_2[PdFe_4(CO)_{12}S_4]$ (**VI**)	+0.025 (150)

[a] All potentials vs SCE. Data obtained from room-temperature CH_3CN solutions with 0.1 M $(n\text{-}Bu_4N)(PF_6)$ as supporting electrolyte. [b] $E_{1/2} = (E_{ox} + E_{red})/2$. $\Delta E = E_{ox} - E_{red}$.

Pyramidal $[Fe_3(CO)_9(\mu_3\text{-}S)]^{2-}$, **Ia**, displays a single quasi-reversible reduction at $E_{1/2} = -0.21$ V (Figure 5a). These observations are in qualitative agreement with a cyclic voltammogram of this cluster reported by others, although their reference electrode was not reported.[8] The cyclic voltammogram of the corresponding selenide, **Ib**, is somewhat more complicated for reasons which are not clear. It has a quasi-reversible reduction at −0.20 V similar to that of the sulfur compound, but also has quasi-reversible reductions at −0.51 and −0.80 V which do not appear in the voltammogram of the sulfide (Figure 5b). These may be due to impurities in solution; however the starting material was analytically pure, and the peaks are reproducible. Another possibility is that the peaks may be due to a follow-up chemical reaction, but we have not been able to gain any further evidence for such a reaction. The bistetrahedral cluster $[Fe_5(CO)_{14}(\mu_3\text{-}S)_2]^{2-}$, **II**, shows two quasi-reversible reductions at 0.017 and −1.60 V. The selenide analog only shows one strong reduction at a more positive potential of 0.060 V (Figure 5c). None of these potentials are indicative of an Fe(II)/Fe(III) couple (vide infra), which implies that the central Fe atom in these clusters is not in a formal divalent state.

All of the compounds which contain a central metal chelated by $[Fe_2(CO)_6S_2]^{2-}$ fragments undergo a single, cleanly reversible reduction. The cluster $[Fe_6S_6(CO)_{12}]^{2-}$, **IVa**, undergoes a 2− to 3− reduction at $E_{1/2} = -1.083$ V (Figure 5d). This is in good agreement with a previous report[12] and can be assigned as the reduction of the central iron dimer core from a formal Fe(III)/Fe(III) state to mixed-valence Fe(II)/Fe(III). This same reduction also occurs in the corresponding selenium compound at $E_{1/2} = -1.01$ V. A general trend that can be noted for all of these complexes is that selenide analogs tend to produce positive potential shifts in the reduction value, meaning that the selenide clusters are more easily reduced than the sulfur analogs. This trend has been observed previously for other iron sulfides and selenide clusters.[22] The Ni and Pd complexes also undergo reversible one-electron reductions at $E_{1/2} = -0.225$ and +0.025 V, respectively (Figure 5e). This couple can be assigned as the reduction of the M^{2+} metal center. The shift to more positive potential upon going from Ni to Pd has been noted previously but has not been fully explained.[22]

The values obtained for these complexes are similar to the well-known metal complexes of tris(1,2-dithiolenes).[23] This

(19) Eisenberg, R. *Prog. Inorg. Chem.* **1970**, *12*, 295.
(20) (a) Sartain, D.; Truter, M. R. *J. Chem. Soc., Chem. Commun.* **1966**, 382. (b) Wing, R. M.; Schlupp, R. L. *Inorg. Chem.* **1970**, *9*, 471.
(21) (a) Ciurli, S.; Ross, P. K.; Scott, M. J.; Yu, S. B.; Holm, R. H. *J. Am. Chem. Soc.* **1992**, *114*, 5415. (b) Ciurli, S.; Carrie, M.; Holm, R. A. *Inorg. Chem.* **1990**, *29*, 3493. (c) Greaney, M. A.; Coyle, C. L.; Pilato, R. S.; Stiefel, E. J. *Inorg. Chim. Acta* **1991** *189*, 81.
(22) Bobrik, M. A.; Laskowski, E. J.; Johnson, R. W.; Gillum, J. M.; Berg, J. M.; Hodgeson, K. O.; Holm, R. H. *Inorg. Chem.* **1978**, *17*, 1402.

leads us to postulate that the $[Fe_2(CO)_6(E)_2]^{2-}$ group can be thought of as a pseudo-dithiolene from both a structural and an electronic viewpoint. Of course, the butterfly compounds do not have an obvious well-developed π system with which to stabilize unusual metal oxidation states. However, both electron-rich sulfide centers and metal carbonyl vertices should serve as modest stabilizers of electron-rich or -poor metal centers as required.

Summary

The reactions of various polysulfides and -selenides with $Fe(CO)_5$ have been systematically explored by varying stoichiometry, conditions and countercations. We originally intended to prepare lighter analogs of the $[Fe_6(CO)_{16}Te_6]^{2-}$ and $[Fe_8(CO)_{20}Te_{10}]^{2-}$ cubanes as models for biological systems, but no evidence for these clusters was found. In fact, the chemistry of the iron carbonyl selenides and sulfides is considerably different from that of the corresponding tellurides. However, we were able to isolate several new iron sulfide and selenide carbonyl clusters in good yield. The controlling factor in these reactions seems to be the length (and hence oxidizing ability) of the starting polychalcogenide chain. It was also found that $[Fe_6S_6(CO)_{12}]^{2-}$ is an excellent $[Fe_2(CO)_6(E)_2]^{2-}$ transfer agent, and a number of heterometal clusters have also been isolated and characterized. It is proposed that the $[Fe_2(CO)_6(E)_2]^{2-}$ butterfly ligands could be viewed as structural analogs of the 1,2-dithiolenes. This postulate is currently being further tested.

Acknowledgment. We are indebted to the National Science Foundation for support of this work. Beverly Hargus was a summer undergraduate participant from Mars Hill College in an NSF-sponsored REU program.

Supporting Information Available: Tables giving complete crystallographic experimental details, distances and angles, positional parameters, anisotropic thermal parameters, and optimized hydrogen atom coordinates and thermal ellipsoid plots of **II** (molecule 2), **III**, and **IVa** (48 pages). Ordering information is given on any current masthead page.

IC940802T

(23) McCleverty, J. A. *Prog. Inorg. Chem.* **1968**, *10* , 84.